

# The Functional Role of the Hemoglobin-Water Interface

Markus Meuwly<sup>\*,†</sup> and Martin Karplus<sup>\*,¶</sup>

<sup>†</sup>*Department of Chemistry, University of Basel, Klingelbergstrasse 80, CH-4056 Basel, Switzerland*

<sup>‡</sup>*Department of Chemistry, Brown University, Providence RI, USA*

<sup>¶</sup>*Department of Chemistry, Harvard University, USA*

<sup>§</sup>*Laboratoire de Chimie Biophysique, ISIS, Université de Strasbourg, 67000 Strasbourg, France*

E-mail: m.meuwly@unibas.ch; marci@tammy.harvard.edu

October 8, 2021

## Abstract

The interface between hemoglobin (Hb) and its environment, in particular water, is of great physiological relevance. Here, results from *in vitro*, *in vivo*, and computational experiments (molecular dynamics simulations) are summarized and put into perspective. One of the main findings from the computations is that the stability of the deoxy, ligand-free T-state ( $T_0$ ) can be stabilized relative to the deoxy R-state ( $R_0$ ) only in sufficiently large simulation boxes for the hydrophobic effect to manifest itself. This effect directly influences protein stability and is operative also under physiological conditions. Furthermore, molecular simulations provide a dynamical interpretation of the Perutz model for Hb function. Results from experiments using higher protein concentrations and realistic cellular environments are also discussed. One of the next

great challenges for computational studies, which as we show is likely to be taken up in the near future, is to provide molecular-level understanding of the dynamics of proteins in such crowded environments.

## Introduction

The human red blood cell (RBC, erythrocyte) contains a complex aqueous solution of hemoglobin, nonhemoglobin proteins, lipids, glucose, electrolytes (mainly  $K^+$ ,  $Na^+$ ,  $Cl^-$ ,  $HCO_3^-$ , and phosphates) and other components. Approximately 97 % of its volume is occupied by water and hemoglobin and that of intracellular water alone of 72 %.<sup>1</sup> Hence, the main interface between hemoglobin and its intracellular environment is with water. Thus, it is essential to be able to describe the interaction between Hb and water for understanding the physiological function of Hb in RBCs.

In this contribution an overview of the current knowledge of the Hb/water interface is provided with an emphasis on the structure and dynamics of the protein and its environment. The solution properties of hemoglobin were already reviewed by Antonini and Brunori in their book published fifty years ago.<sup>2</sup> At the time the solution structure of the protein, its oligomerization state and the behaviour in solutions with different ionic strengths were of particular interest. A protein's solvent environment and its chemical composition can change its effects from acting as plasticizers (e.g. water) to being stabilizers (e.g. trehalose or glycerol). At a molecular level this is further complicated by the fact that protein side chains can switch between conformational substates and that certain such motions can be prevented. For example, for lysozyme it was shown experimentally that the internal dynamics is activated when the environment changes from pure glycerol (which is a stabilizer) by increasing the level of hydration, because water is a plasticizer.<sup>3</sup> More generally it has been found that protein dynamics is *slaved* to solvent fluctuations.<sup>4</sup> Increased hydration has also been found to affect internal motions.<sup>5</sup> Hence, it is essential to better understand the interplay between

solvent structure and dynamics and the protein dynamics coupled to it and whether this influences the biological function in a physiological context.

A first dynamical transition of the internal dynamics of proteins between “low amplitude motion” and more “diffusive motion” occurs between 180 K and 220 K<sup>6</sup> although for the protein thaumatin a transition at 110 K has been reported.<sup>7</sup> This “glass transition” was investigated by using quasi-inelastic neutron scattering experiments or Mössbauer spectroscopy.<sup>8</sup> Experiments on Hb in RBCs have reported an “elastomeric transition” between a gel- and a fluid-like phase.<sup>9</sup> At a temperature of 310 K, human RBCs were found to undergo a sudden change from blocking to passing through micropipettes. This behavior was associated with a gel-to-fluid phase transition<sup>9</sup> which is also related to the known increase in viscosity of highly concentrated Hb. Subsequent experiments on RBCs from different organisms revealed that such a transition involves Hb in all cases and that, more surprisingly, the transition temperature is correlated with the body temperature of the respective species.<sup>10</sup>

It was hypothesized that the drop in viscosity with subsequent changes for cellular passage through micropipettes is caused by protein aggregation.<sup>9</sup> Concomitantly, Hb shows a pronounced loss of its  $\alpha$ -helical content at body temperature, not only for human Hb, but also for several other species.<sup>11</sup> It was proposed<sup>12</sup> that this is due to an increased amplitude of the sidechain motions. This triggers unfolding of the helical structure accompanied by an increase in surface hydrophobicity, which eventually leads to protein aggregation. Experimentally, this was investigated by temperature-dependent incoherent quasielastic neutron scattering on whole red blood cells.<sup>10</sup> Such experiments are able to separate global and internal protein motions. It was found that the amplitudes of protein side-chain motions increased close to the body temperature of different species, such as monotremes (305 K) and humans (311 K) with the difference due to amino acid substitutions.

# The Role of Water for the Stability of Hemoglobin

Hemoglobin (Hb) is one of the most widely studied proteins due to its essential role in transporting oxygen from the lungs to the tissues. Binding of molecular oxygen,  $O_2$ , at the heme-iron is the physiologically relevant step for oxygen transport. Oxygen homeostasis<sup>13</sup> at the molecular level can be described as the dynamic equilibrium between  $O_2$ -bound and ligand-free Hb at one of the four heme-iron atoms and depends on the local  $O_2$  concentration. The self-regulation of oxygen homeostasis is reflected in protein allostery,<sup>14</sup> the capacity of proteins such as Hb to modulate their affinity towards a physiological target (here  $O_2$ ) by structural adaptations upon binding or removal of another ligand (here  $O_2$ ) at a different binding site. In other words, allostery is the molecular embodiment of homeostasis at the cellular level. The two most important structural states of Hb are the deoxy structure ( $T_0$ ), which is stable when no ligand (subscript “0”) is bound to the heme-iron, and the oxy structure ( $R_4$ ), which is stable when each of the four heme groups have a ligand (subscript “4”), such as oxygen, bound to them, see Figure 1 for the structure of the active site including the heme, the surrounding histidine residues, and the bound  $O_2$  ligand (right panel). The state with the quaternary structure of  $R_4$ , but with no heme-bound ligands is the  $R_0$  state. Despite strong experimental evidence<sup>15</sup> that  $T_0$  is significantly more stable than  $R_0$ , with an equilibrium constant of  $K_{\frac{T_0}{R_0}} = 6.7 \times 10^5$ , molecular dynamics (MD) simulations appeared to indicate that the  $R_0$  state is more stable than  $T_0$ . Specifically, simulations started with hemoglobin in its  $T_0$  state have been found to undergo a spontaneous transition into the  $R_0$  state on sub- $\mu$ s time scales.<sup>16,17</sup> Understanding the molecular details of this discrepancy between the experimentally measured and simulated relative stabilities of the  $R_0$  and  $T_0$  states is essential for establishing the reliability of simulation-based studies of Hb and other large biomolecules.

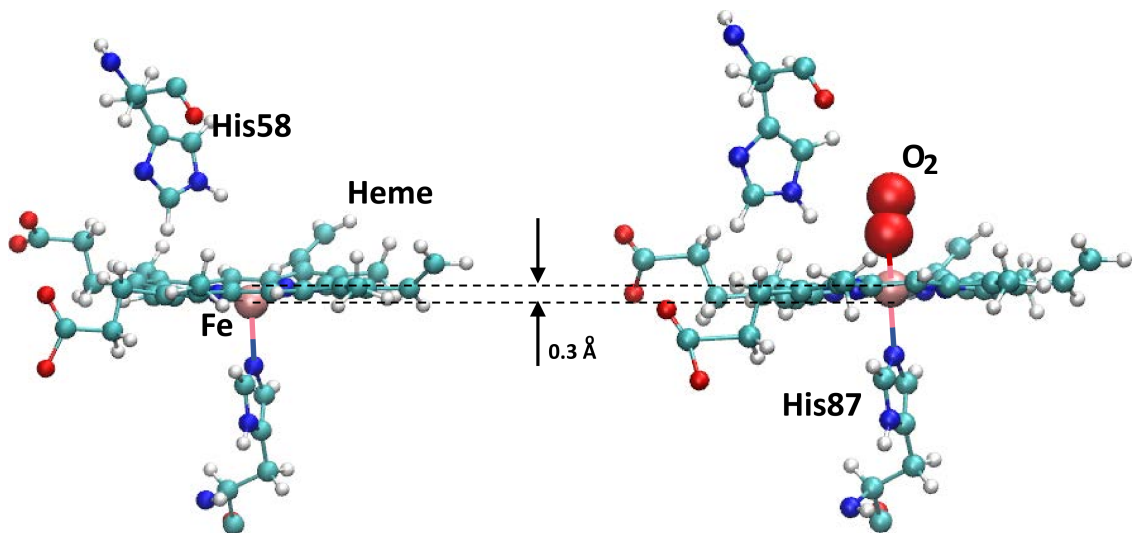


Figure 1: The active site of Hemoglobin with the heme-group (CPK), the heme-iron (light red sphere), the  $O_2$  ligand (dark red spheres), and the two histidine residues surrounding the active site with His87 covalently bound to the heme-iron. The position of the iron atom is  $\sim 0.3$  Å below the average heme plane for the 5-coordinate heme (left) and in the heme plane for 6-coordinate heme (right).

In a recent set of MD simulations it was found that the  $T_0 \rightarrow R_0$  transition rate depends sensitively on the size of the simulation box.<sup>18</sup> The simulations were initialized with Hb in the  $T_0$  state and immersed in a periodically replicated cubic solvent box with side lengths of 75 Å, 90 Å, and 120 Å. In such boxes transitions towards the R-state structure were observed after 130 ns, 480 ns, and 630 ns, respectively. By contrast, in a water box with side-length 150 Å (top row Figure 2), Hb remained in its  $T_0$  state for the entirety of a 1.2 $\mu$ s simulation. Extrapolation of this trend suggests that  $T_0$  is the thermodynamically stable state in this water box.

The results also suggested that such a large box is required for the hydrophobic effect, which stabilizes the  $T_0$  tetramer, to be manifested. Hydrophobicity is the tendency of a solute (here Hb) to pack with itself and to exclude water molecules. In other words, the solute and water segregate which leads to maximization of hydrogen bonds between water molecules while minimizing the contact area between the solute and water. The hydrophobic effect is one of the main driving forces in the formation of biological interfaces, including cell membranes

and vesicles and thus is essential for life.<sup>19</sup>

The importance of the hydrophobic effect as an organizing “force” in biological systems has been recognized for quite some time. Hydrophobicity has been discussed and established as an important driver in protein folding or for the compartmentalization of cells.<sup>19</sup> However, the hydrophobic effect is also prevalent in everyday life (in the function of detergents or emulsions), in materials sciences, adhesion, and confinement.<sup>20</sup> One of the findings particularly relevant to the present discussion is the dependence of hydration of a hydrophobe on its size, see Figure 2 bottom row. Considering an idealized spherical cavity of radius  $R$  it was shown that the density of water a distance  $r$  from the surface of the cavity depends sensitively on its size. For a small cavity ( $R \sim 4 \text{ \AA}$ , the size of methane,  $\text{CH}_4$ ) the water density adjacent to the cavity is larger by a factor of two than the bulk density of water because water attempts to maintain a H-bonding network as strong and dense as possible.<sup>20</sup> This changes with increasing size of the cavity. For a cavity the size of hemoglobin ( $R \sim 25 \text{ \AA}$ ) solvent density around the protein is depleted and approaches bulk density asymptotically without evident structure in the radial distribution function,  $g(r)$ , see bottom Figure 2. These findings are consistent with earlier MD simulations of hydrophobic hydration of melittin.<sup>21</sup> In these simulations it was found that depending on the local curvature of the protein (e.g. a “flat”  $\beta$ -sheet region compared with a “pointed” turn), hydrophobic residues of even the same chemical type show different water hydration shells due to local constraints on hydrogen bonding which lead to different orientational water structures. In other words: flat surfaces impose different constraints on the water H-bonding patterns than surfaces with large curvature. The predicted overall behaviour of the radial distribution function from model studies, as shown in the bottom panels of Figure 2, is consistent with those found from the atomistic simulations for Hb, see middle panel of Figure 2.

These findings demonstrate that the global and local structure of the solute also influence the

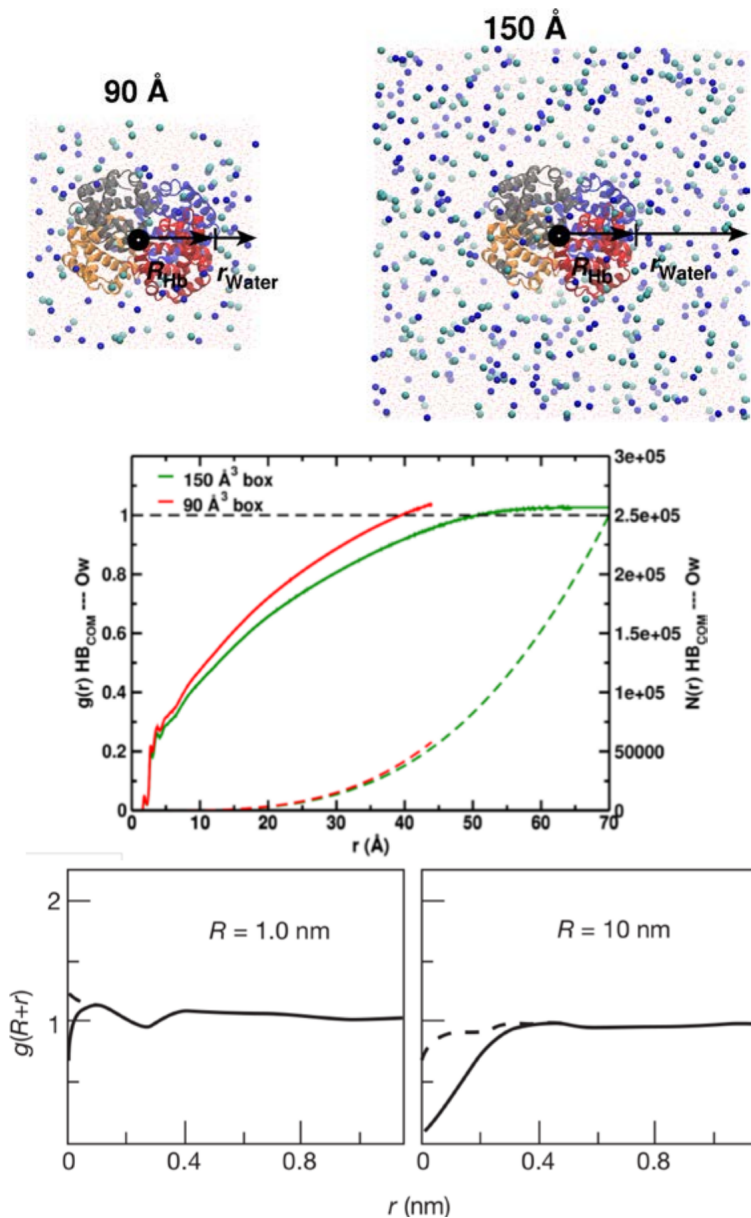


Figure 2: Hydration structure depending on the size of the solute. Top: Hb in a 90 Å (left) and 150 Å (right) solvent box together with the ions (blue and cyan spheres) to give an ionic strength of 0.15 M. Middle: solvent structure around Hb for the two different box sizes; the solid lines are the radial distribution function,  $g(r)$ , and the dotted lines show the total number of water molecules,  $N(r)$ , up to a distance  $r$  from the surface of the solute. Bottom: Predictions of the solvent structure from model studies<sup>20</sup> depending on the size  $R$  of the solute: 10 Å (left) and 100 Å (right). The solid line is for an ideal hydrophobic solute and the dashed line includes van der Waals attractions between the solute and water. Figure adapted with permission from Ref.<sup>18</sup> with the two bottom panels from Ref.<sup>20</sup>

global and local hydration which, in turn, affect the thermodynamic stability of the solute. Because the root mean squared difference between the  $T_0$  and the  $R_4$  structures of Hb is  $\sim 5$  Å, their hydration is also expected to differ. This supports the observed dependence of the thermodynamic stability of  $T_0$  vs.  $R_0$ , where  $R_0$  is expected to be  $R_4$ -like, on the size of the water box as found from the MD simulations.<sup>18</sup> While the statistical significance of these findings has been a topic of recent discussion in the literature,<sup>22,23</sup> the dynamic stability of the  $T_0$  state exhibits a clear and systematic dependence on the size of the solvent box. The differences in the degree of hydration between the T- and the R-states is also consistent with earlier work based on individual X-ray structures.<sup>24</sup> It is well established that the  $\alpha_1\beta_2$  and  $\alpha_2\beta_1$  interfaces in Hb are large and closely packed. Although the allosteric transition has been shown to be more complex,<sup>25</sup> it can be described as a  $\sim 15^\circ$  rotation of the  $\alpha_1\beta_1$  dimer relative to the  $\alpha_2\beta_2$  dimer. The T $\rightarrow$ R transition also involves breaking of several salt bridges, in accord with the Perutz mechanism.<sup>26,27</sup> Concomitantly, the buried surface of the R-state is reduced by  $\sim 700$  Å<sup>2</sup> as compared with the T-state. Based on the relationship between solvent accessible surface area and the associated hydrophobic contribution to the free energy,<sup>28</sup> burial of additional protein surface will differentially stabilize the T-state relative to the R-state. Hence, the decrease in the protein surface exposed to the solvent suggests that hydrophobic effects should stabilize the T-state. Further analysis is required to provide conclusive evidence of the role of the hydrophobic effect and to reveal the mechanistic origin of the dependence of the thermodynamic stability of the  $T_0$  state, relative to the  $R_0$  state, on the simulation box size. A related interesting and challenging aspect concerns the question of whether the solvent water follows the conformational T $\rightarrow$ R transition or whether water drives this transition. It is also possible that during different phases of this transition the roles of solvent and solute switch or that it is more meaningful to consider the solvent-solute system as a whole.

It is of interest to note that recent work on the A $\beta$  peptide, which is the main component of



amyloid plaques involved in Alzheimer’s disease, found that different solvent box sizes yield similar radius of gyration, secondary structure, intrapeptide, and peptide-water hydrogen bonds.<sup>30</sup> However, of considerable interest for the present discussion, it was reported that the hydrophobic surface area and exposure of the backbone conformations depend significantly and sensitively on the solvent box size, irrespective of the force field used in the simulations.<sup>30</sup> Similarly, MD studies of nanoparticle diffusion also reported differences in the hydration depending on the size of the solvent box.<sup>31</sup> For Hb as the solute the water diffusion coefficients also depends on the size of the simulation box, see Figure 3. It is found that with increasing box size the diffusivity of water for the system including hemoglobin approaches that of the solvent alone. Finally, following a tangential approach to the problem by use of quasichemical theory it was reported that both hydrophilic and hydrophobic contributions to hydration depend on system size. They are predicted to decrease with increasing system size. The net hydration free energy benefits somewhat from the compensation of hydrophilic and hydrophobic contributions which is akin to entropy/enthalpy compensation.<sup>32,33</sup> Neverthe-

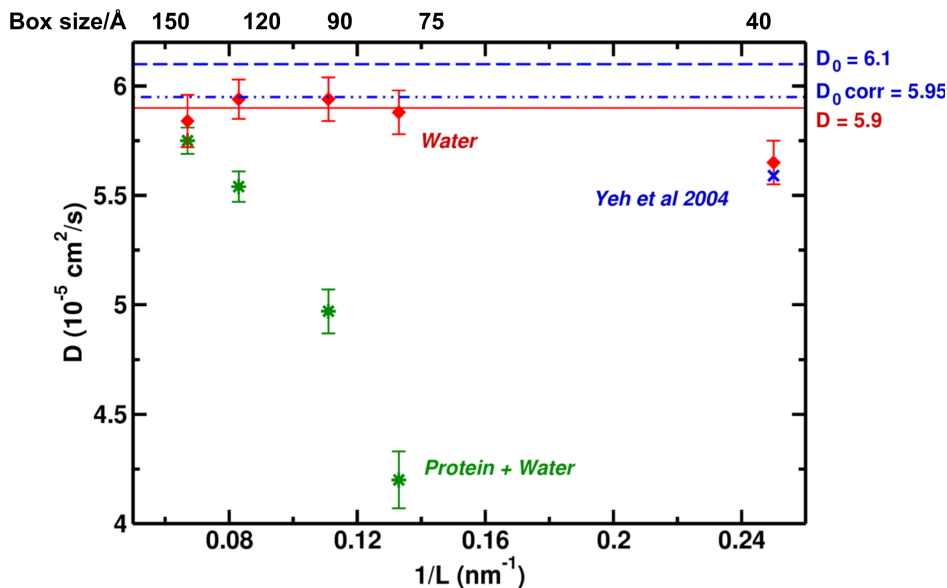


Figure 3: The dependence of the water diffusivity on the size of the simulation system with (green symbols) and without (red symbols) Hb as the solute. Direct comparison for the smallest simulation box with that from the literature<sup>29</sup> is favourable. Figure adapted with permission from Ref.<sup>18</sup>

less, a large system appears necessary to describe correctly the balance of these contributions to the hydration of the macromolecule.<sup>34</sup>

More molecularly resolved and quantitative work has been done to understand the local hydration of Hb in its  $T_0$  and  $R_0$  states.<sup>35</sup> For this, the local hydrophobicity (LH) was evaluated<sup>36,37</sup> along MD trajectories of the two conformational states in differently sized water boxes. The local hydrophobicity can be viewed as a generalization of a radial distribution function in that it provides information about both the presence *and* orientation of water molecules at an interface. Such an analysis for the  $T_0$  and  $R_0$  states of Hb found that the breaking and formation of salt bridges at the  $\alpha_1\beta_2$  and  $\alpha_2\beta_1$  interface is accompanied by changes in LH.

The above provides a molecular view of the Perutz mechanism which is based on a two-state model involving an equilibrium between the T- and the R-states.<sup>26,38</sup> In the Perutz model the  $T_0$ -state is “tense”, constrained by salt bridges between the C-termini of the four subunits and it has a low oxygen affinity with no ligands bound, whereas the  $R_4$ -state is “relaxed”, the salt bridges are broken and ligands are bound to the heme-irons. The  $T_0$ -state has the (5-coordinated) heme-iron out of plane displaced towards the proximal histidine His87, see Figure 1, whereas in the  $R_4$  state the heme-iron is in the plane and is six-coordinated with the ligand occupying the remaining free valence as shown in Figure 1. Every heme-iron atom is coordinated to a histidine residue at its distal site (“below the heme plane”). The histidine residues are His87 in the  $\alpha$ -chains and His92 in the  $\beta$ -chains. Because these histidine residues are part of the F-helix that is linked to the E-helix (containing the proximal histidine residue) forming a loop, motion at the distal side of each subunit can be efficiently transduced to other relevant parts of the protein.<sup>39</sup> The  $T_0/R_4$  equilibrium it thought to be governed primarily by the position of the iron atoms relative to the porphyrin and the salt bridge stability and dynamics is considered to be linked to the distal histidines.<sup>26,27</sup> This

interplay between ligand binding, local and global conformational changes, the change in interface exposed to the solvent and subsequent rearrangement of solvent leads to a logical chain of events spanning various length scales (from atomic to mesoscopic) that govern Hb function.

For Hb in cubic water boxes with 90 Å and 120 Å edge length it was found that simulations initialized in the  $T_0$  state decay to known but different intermediate structures upon destabilization of the  $\alpha\beta$  interface following a decrease in LH; i.e. as a consequence of reduced water density or change of water orientation at the protein/water interface.<sup>35</sup> This is in line with earlier simulations<sup>18</sup> that reported a reduced number of water-water hydrogen bonds in smaller simulation boxes which shifts the equilibrium between water-protein and water-water contacts and changes the activity of water. Interestingly, for decreasing box sizes, simulations for the A $\beta$  peptide reported a pronounced increase in the hydrophobic surface area<sup>30</sup> and studies of protein G found an increase in the hydrophobic contribution due to a decrease in solvent density fluctuations as the system size decreases.<sup>34</sup> This is consistent with studies for Hb that found larger hydrophobic exposure in smaller simulation boxes.<sup>35</sup>

## **Characterization of the Protein/Water Interface from Measurements on RBCs**

In contrast to studies of individual macromolecules, such as Hb, in aqueous solution containing adequate concentrations of anions and cations (see previous sections), proteins in a realistic cellular environment experience extreme crowding.<sup>40</sup> Hence, although the above studies are of interest to better understand the physical behaviour of complex macromolecules at a molecular level, they are not necessarily directly relevant to the behaviour of proteins under physiological conditions.

A notable experiment<sup>41</sup> determined the diffusivity of water in Hb/water mixtures at protein concentrations of  $\sim 330$  mg/mL, which is representative of the crowded cellular environment with protein concentrations of up to 400 mg/mL. Using quasielastic incoherent neutron scattering (QENS) to probe the water dynamics of RBCs in D<sub>2</sub>O and H<sub>2</sub>O buffer, the cytoplasmic dynamics of H<sub>2</sub>O was separated from membrane and macromolecular dynamics. The difference in the two signals is dominated by the water dynamics because hydrogen nuclei have an incoherent scattering cross section that is  $\sim 40$  times larger than that of macromolecules or deuterium. The translational diffusion of cellular water was found to be nearly identical to that of H<sub>2</sub>O buffer which is consistent with the results from MD simulations if sufficiently large solvent boxes are used, see Figure 3. However, this finding is surprising for cellular environments for three reasons. First, the average separation of macromolecules in a crowded cellular environment is of the order of 10 Å which corresponds to only  $\sim 3$  layers of water molecules. Second, NMR experiments<sup>42</sup> and MD simulations<sup>43</sup> have found that the reorientation dynamics of water on the protein surface is slowed down by a factor of 2 to 3 compared with water in the bulk. Third, time resolved fluorescence spectroscopy reported that a significant fraction of the water molecules is slowed down by an order of magnitude.<sup>44</sup> Although in fact, the notion that the dynamics of water adjacent to a protein surface differs from that in the bulk dates back at least 60 years,<sup>45</sup> there is as yet no explanation for the high diffusivity of cellular water.

Much effort has gone into characterizing the behaviour of Hb in RBCs.<sup>46</sup> Of particular relevance is the understanding of the sensitivity of the volume of RBCs to changes in the osmolality of the surrounding medium. Such effects were referred to as “anomalous osmotic behaviour” of RBCs.<sup>47</sup> Interestingly, the molecular explanation for the apparent anomaly is a cooperative effect by which the total charge of Hb decreases with increased Hb concentration.<sup>48</sup>

## Relevance of *In Vitro* Studies to Physiology

As noted above, in a cellular environment the spatial separation between proteins is of the order of 10 Å. This differs considerably from most MD studies that investigate one or a few proteins in solution. Similarly, NMR experiments are carried out under dilute conditions that avoid clustering of the proteins. Hence, the question arises in what sense such *in vitro* studies are relevant to the situation encountered *in vivo*.

A first obvious difference, as already mentioned, is the “crowding” encountered in real cells. Typically, physico-chemical experiments aim at *reducing* the complexity in order to obtain *specific* information about the system of interest - here the energetics and dynamics of Hb. However, crowding and the presence of multiple interaction partners generally makes the interpretation of experiments on RBCs difficult. For example, when using infrared spectroscopy to probe site-specific dynamics in a protein much effort is spent in finding molecules that absorb in a frequency range that is largely devoid of responses from the protein.<sup>49</sup> This range extends from  $\sim 1800 \text{ cm}^{-1}$  to  $\sim 2900 \text{ cm}^{-1}$ . Hence, spectroscopic probes such as -CN,<sup>50</sup> -SCN,<sup>51</sup> or  $\text{N}_3$ <sup>52-54</sup> which absorb between  $2000 \text{ cm}^{-1}$  and  $2300 \text{ cm}^{-1}$  are ideal reporters since all signals in this frequency range can be unambiguously assigned to the reporter groups.

One significant study directly probed the water dynamics in a cellular environment.<sup>55</sup> Contradicting the view that a substantial fraction of cell water is strongly perturbed, it was found that  $\sim 85 \%$  of cell water in *E. coli* and in the extreme halophile *Haloarcula marismortui* had bulk-like dynamics, consistent with the results in Figure 3. The remaining  $\sim 15 \%$  of cell water interacts directly with biomolecular surfaces and is motionally retarded by a factor  $15 \pm 3$  on average, corresponding to a rotational correlation time of 27 ps. This dynamic

perturbation is three times larger than for small monomeric proteins in solution, a difference that was attributed to secluded surface hydration sites in supramolecular assemblies.

More recently, all atom MD simulations of the *Mycoplasma genitalium* (Mg), the simplest bacterium, with a genome of 470 genes versus *E. coli*, which has about 4600 genes, have been performed.<sup>56</sup> They included all molecular components (i.e. proteins, RNA, metabolites, ion, and water) explicitly in atomic detail with a total of  $\sim 104$  million atoms. The system was simulated for 20  $\mu$ s. Even with this short simulation time some interesting results were obtained; e.g., partial denaturation due to protein-protein interactions occurred and macromolecular diffusion was slowed down.

Another example of the differences between *in vivo* and *in vitro* studies was found for the production of recombinant adeno-associated viruses.<sup>57</sup> Although this example is not related to hemoglobin *per se*, it nicely illustrates that the behaviour of a complex system (such as a multimeric protein) depends on the structure and composition of its environment (i.e., in a cell or under idealized laboratory conditions). For the production of such viruses, all conditions were maintained identical except for the host cell species in which they were grown. Interestingly, the post translational modifications of the viruses expressed in the two different cell types differed and the sites at which methylation occurred also depended on the cell line that was used. It was concluded that virus receptor binding, trafficking, or expression kinetics can depend on the method used to grow the virus.

## Summary

The present work highlights the importance of a molecular-level understanding of the interface between hemoglobin and its environment, notably water, under *in vivo* and *in vitro*

conditions. In cellular environments, such as RBCs, crowding is the main difference when compared with more idealized realizations of a system *in vitro* in most computational and physico-chemical experiments. Although following such “divide-and-conquer” approaches has provided remarkable insights into the dynamics and thermodynamics of complex systems, their relevance to those experienced under physiological conditions needs to be examined in detail. The finding that 85 % of the water in cells behave like bulk water and only 15 % has slowed its diffusion by one order of magnitude suggests that laboratory experiments and molecular simulations with slight modifications (“crowders”) should be able to emulate many aspects of real-cell environments without unduly increasing the complexity of the system investigated. This is even more likely to be a meaningful approach as simulations for Hb carried out in sufficiently large solvent boxes confirm these findings. Bridging the gap between idealized single-molecule scenarios typically considered in current laboratory and simulation-based experiments and the crowded cellular environments is a challenge that will be taken up in the near future to obtain a molecular-level understanding of complex biological systems, including living cells.

## Acknowledgment

The authors thank Adam Willard for insightful comments and thoughtful correspondence. Support by the Swiss National Science Foundation through grants 200021-117810, the NCCR MUST (to MM), and the University of Basel is acknowledged. The support of MK by the CHARMM Development Project is gratefully acknowledged.

## References

- (1) Levin, R.; Cravalho, E.; Huggins, C. Effect of hydration on the water content of human erythrocytes. *Biophys. J.* **1976**, *16*, 1411–1426.
- (2) Antonini, E.; Brunori, M. *Hemoglobin and Myoglobin in Their Reactions with Ligands*; North-Holland Publ. Co., Amsterdam, 1971.
- (3) Paciaroni, A.; Cinelli, S.; Onori, G. Effect of the environment on the protein dynamical transition: a neutron scattering study. *Biophys. J.* **2002**, *83*, 1157–1164.
- (4) Fenimore, P. W.; Frauenfelder, H.; McMahon, B. H.; Parak, F. G. Slaving: solvent fluctuations dominate protein dynamics and functions. *Proc. Natl. Acad. Sci.* **2002**, *99*, 16047–16051.
- (5) Smith, J.; Kuczera, K.; Tidor, B.; Doster, W.; Cusack, S.; Karplus, M. Internal dynamics of globular proteins: comparison of neutron scattering measurements and theoretical models. *Physica B: Condensed Matter* **1989**, *156*, 437–443.
- (6) Doster, W.; Cusack, S.; Petry, W. Dynamical transition of myoglobin revealed by inelastic neutron scattering. *Nature* **1989**, *337*, 754–756.
- (7) Kim, C. U.; Tate, M. W.; Gruner, S. M. Protein dynamical transition at 110 K. *Proc. Natl. Acad. Sci.* **2011**, *108*, 20897–20901.
- (8) Achterhold, K.; Keppler, C.; Ostermann, A.; Van Bürck, U.; Sturhahn, W.; Alp, E.; Parak, F. Vibrational dynamics of myoglobin determined by the phonon-assisted Mössbauer effect. *Phys. Rep.* **2002**, *65*, 051916.
- (9) Artmann, G.; Kelemen, C.; Porst, D.; Buldt, G.; Chien, S. Temperature transitions of protein properties in human red blood cells. *Biophys. J.* **1998**, *75*, 3179–3183.



- (10) Stadler, A. M.; Digel, I.; Artmann, G.; Embs, J. P.; Zaccai, G.; Buldt, G. Hemoglobin dynamics in red blood cells: correlation to body temperature. *Biophys. J.* **2008**, *95*, 5449–5461.
- (11) Zerlin, K. F. T.; Kasischke, N.; Digel, I.; Maggakis-Kelemen, C.; Artmann, A. T.; Porst, D.; Kayser, P.; Linder, P.; Artmann, G. M. Structural transition temperature of hemoglobins correlates with species' body temperature. *Eur. Biophys. J.* **2007**, *37*, 1–10.
- (12) Digel, I.; Maggakis-Kelemen, C.; Zerlin, K.; Linder, P.; Kasischke, N.; Kayser, P.; Porst, D.; Artmann, A. T.; Artmann, G. Body temperature-related structural transitions of monotremal and human hemoglobin. *Biophys. J.* **2006**, *91*, 3014–3021.
- (13) Semenza, G. L. Oxygen homeostasis. *Wiley Interdisciplinary Reviews: Systems Biology and Medicine* **2010**, *2*, 336–361.
- (14) Cui, Q.; Karplus, M. Allostery and cooperativity revisited. *Prot. Sci.* **2008**, *17*, 1295–1307.
- (15) Edelstein, S. Extensions of the allosteric model for haemoglobin. *Nature* **1971**, *230*, 224–227.
- (16) Hub, J. S.; Kubitzki, M. B.; de Groot, B. L. Spontaneous Quaternary and Tertiary T-R Transitions of Human Hemoglobin in Molecular Dynamics Simulation. *PLoS. Comput. Biol.* **2010**, *6*, e1000774.
- (17) Yusuff, O. K.; Babalola, J. O.; Bussi, G.; Raugei, S. Role of the Subunit Interactions in the Conformational Transitions in Adult Human Hemoglobin: An Explicit Solvent Molecular Dynamics Study. *J. Phys. Chem. B* **2012**, *116*, 11004–11009.
- (18) El Hage, K.; Hedin, F.; Gupta, P. K.; Meuwly, M.; Karplus, M. Valid molecular dy-

- namics simulations of human hemoglobin require a surprisingly large box size. *eLife* **2018**, *7*, e35560.
- (19) Tanford, C. The hydrophobic effect and the organization of living matter. *Science* **1978**, *200*, 1012–1018.
- (20) Chandler, D. Interfaces and the driving force of hydrophobic assembly. *Nature* **2005**, *437*, 640–647.
- (21) Cheng, Y.; Rossky, P. Surface topography dependence of biomolecular hydrophobic hydration. *Nature* **1998**, *392*, 696–699.
- (22) Gapsys, V.; de Groot, B. L. Comment on ‘Valid molecular dynamics simulations of human hemoglobin require a surprisingly large box size’. *eLife* **2019**, *8*, e44718.
- (23) El Hage, K.; Hedin, F.; Gupta, P. K.; Meuwly, M.; Karplus, M. Response to comment on ‘Valid molecular dynamics simulations of human hemoglobin require a surprisingly large box size’. *eLife* **2019**, *8*, e45318.
- (24) Lesk, A.; Janin, J.; Wodak, S.; Chothia, C. Hemoglobin - The surface buried between the  $\alpha_1\beta_1$  and  $\alpha_2\beta_2$  dimers in the deoxy and oxy structures. *J. Mol. Biol.* **1985**, *183*, 267–270.
- (25) Fischer, S.; Olsen, K. W.; Nam, K.; Karplus, M. Unsuspected pathway of the allosteric transition in hemoglobin. *Proc. Natl. Acad. Sci.* **2011**, *108*, 5608–5613.
- (26) Perutz, M. F. Stereochemistry of Cooperative Effects in Haemoglobin. *Nature* **1970**, *228*, 726–734.
- (27) Perutz, M. F.; Wilkinson, A.; Paoli, M.; Dodson, G. The stereochemical mechanism of the cooperative effects in hemoglobin revisited. *Ann. Rev. Biophys. Biomol. Struct.* **1998**, *27*, 1–34.

- (28) Chothia, C. Hydrophobic bonding and accessible surface area in proteins. *Nature* **1974**, *248*, 338–339.
- (29) Yeh, I.; Hummer, G. System-size dependence of diffusion coefficients and viscosities from molecular dynamics simulations with periodic boundary conditions. *J. Phys. Chem. B* **2004**, *108*, 15873–15879.
- (30) Mehra, R.; Kepp, K. P. Cell size effects in the molecular dynamics of the intrinsically disordered A $\beta$  peptide. *J. Chem. Phys.* **2019**, *151*.
- (31) Cui, A. Y.; Cui, Q. Modulation of Nanoparticle Diffusion by Surface Ligand Length and Charge: Analysis with Molecular Dynamics Simulations. *J. Phys. Chem. B* **2021**,
- (32) Sharp, K. Entropy-enthalpy compensation: Fact or artifact? *Prot. Sci.* **2001**, *10*, 661–667.
- (33) Chodera, J. D.; Mobley, D. L. Entropy-enthalpy compensation: role and ramifications in biomolecular ligand recognition and design. *Ann. Rev. Biophys.* **2013**, *42*, 121–142.
- (34) Asthagiri, D.; Tomar, D. S. System size dependence of Hydration-Shell occupancy and its implications for assessing the hydrophobic and hydrophilic contributions to hydration. *J. Phys. Chem. B* **2020**, *124*, 798–806.
- (35) Pezzella, M.; El Hage, K.; Niesen, M. J.; Shin, S.; Willard, A. P.; Meuwly, M.; Karplus, M. Water dynamics around proteins: T- and R-States of Hemoglobin and Melittin. *J. Phys. Chem. B* **2020**, *124*, 6540–6554.
- (36) Willard, A. P.; Chandler, D. Instantaneous liquid interfaces. *J. Phys. Chem. B* **2010**, *114*, 1954–1958.
- (37) Shin, S.; Willard, A. P. Characterizing hydration properties based on the orientational structure of interfacial water molecules. *J. Chem. Theor. Comput.* **2018**, *14*, 461–465.

- (38) Antonini, E.; Brunori, M. *Hemoglobin and Myoglobin in Their Reactions with Ligands*; North-Holland Publ. Co., Amsterdam, 1971; pp Chapter 14, Section 14.3.4.
- (39) Kachalova, G. S.; Popov, A. N.; Bartunik, H. D. A steric mechanism for inhibition of CO binding to heme proteins. *Science* **1999**, *284*, 473–476.
- (40) Zhou, H.-X.; Rivas, G.; Minton, A. P. Macromolecular crowding and confinement: Biochemical, biophysical, and potential physiological consequences. *Ann. Rev. Biophys.* **2008**, *37*, 375–397.
- (41) Stadler, A. M.; Embs, J. P.; Digel, I.; Artmann, G. M.; Unruh, T.; Buldt, G.; Zaccai, G. Cytoplasmic water and hydration layer dynamics in human red blood cells. *J. Am. Chem. Soc.* **2008**, *130*, 16852–16853.
- (42) Mattea, C.; Qvist, J.; Halle, B. Dynamics at the protein-water interface from  $^{17}\text{O}$  spin relaxation in deeply supercooled solutions. *Biophys. J.* **2008**, *95*, 2951–2963.
- (43) Sterpone, F.; Stirnemann, G.; Laage, D. Magnitude and molecular origin of water slowdown next to a protein. *J. Am. Chem. Soc.* **2012**, *134*, 4116–4119.
- (44) Pal, S. K.; Peon, J.; Zewail, A. H. Biological water at the protein surface: dynamical solvation probed directly with femtosecond resolution. *Proc. Natl. Acad. Sci.* **2002**, *99*, 1763–1768.
- (45) Bernal, J. The structure of water and its biological implications. Symposia of the Society for Experimental Biology. 1965; pp 17–32.
- (46) Longeville, S.; Stingaciu, L.-R. Hemoglobin diffusion and the dynamics of oxygen capture by red blood cells. *Sci. Rep.* **2017**, *7*, 1–10.
- (47) Savitz, D.; Sidel, V. W.; Solomon, A. Osmotic properties of human red cells. *J. Gen. Physiol.* **1964**, *48*, 79–94.

- (48) Gary-Bobo, C.; Solomon, A. Properties of hemoglobin solutions in red cells. *J. Gen. Physiol.* **1968**, *52*, 825–853.
- (49) Koziol, K. L.; Johnson, P. J. M.; Stucki-Buchli, B.; Waldauer, S. A.; Hamm, P. Fast Infrared Spectroscopy of Protein Dynamics: Advancing Sensitivity and Selectivity. *Curr. Op. Struct. Biol.* **2015**, *34*, 1–6.
- (50) Zimmermann, J.; Thielges, M. C.; Seo, Y. J.; Dawson, P. E.; Romesberg, F. E. Cyano Groups as Probes of Protein Microenvironments and Dynamics. *Angew. Chem. Intern. Ed.* **2011**, *50*, 8333–8337.
- (51) van Wilderen, L. J. G. W.; Kern-Michler, D.; Mueller-Werkmeister, H. M.; Bredenbeck, J. Vibrational dynamics and solvatochromism of the label SCN in various solvents and hemoglobin by time dependent IR and 2D-IR spectroscopy. *PCCP* **2014**, *16*, 19643–19653.
- (52) Bloem, R.; Koziol, K.; Waldauer, S. A.; Buchli, B.; Walser, R.; Samatanga, B.; Jelezarov, I.; Hamm, P. Ligand Binding Studied by 2D IR Spectroscopy Using the Azido-homoalanine Label. *J. Phys. Chem. B* **2012**, *116*, 13705–13712.
- (53) Salehi, S. M.; Koner, D.; Meuwly, M. Vibrational Spectroscopy of N<sub>3</sub>–in the Gas and Condensed Phase. *J. Phys. Chem. B* **2019**, *123*, 3282–3290.
- (54) Salehi, S. M.; Meuwly, M. Site-selective dynamics of azidolysosome. *J. Chem. Phys.* **2021**, *154*, 165101.
- (55) Persson, E.; Halle, B. Cell water dynamics on multiple time scales. *Proc. Natl. Acad. Sci.* **2008**, *105*, 6266–6271.
- (56) Yu, I.; Mori, T.; Ando, T.; Harada, R.; Jung, J.; Sugita, Y.; Feig, M. Biomolecular interactions modulate macromolecular structure and dynamics in atomistic model of a bacterial cytoplasm. *eLife* **2016**, *5*, e19274.

- (57) Rumachik, N. G.; Malaker, S. A.; Poweleit, N.; Maynard, L. H.; Adams, C. M.; Leib, R. D.; Cirolia, G.; Thomas, D.; Stamnes, S.; Holt, K. Methods matter: standard production platforms for recombinant AAV produce chemically and functionally distinct vectors. *Mol. Therap. - Meth. Clin. Devel.* **2020**, *18*, 98–118.